

1 **Automated segmentation and quantitative analysis of**  
2 **organelle morphology, localization and content using**  
3 **CellProfiler**

4

5 Sebastiaan N.J. Laan<sup>1,2</sup>, Richard J. Dirven<sup>1</sup>, Jeroen Eikenboom<sup>1</sup> and Ruben Bierings<sup>2</sup> for the  
6 SYMPHONY consortium

7

8 <sup>1</sup>Internal Medicine, Division of Thrombosis and Hemostasis, Leiden University Medical Center,  
9 Leiden, The Netherlands;

10 <sup>2</sup>Hematology, Erasmus University Medical Center, Rotterdam, The Netherlands.

11

12 Running title: Automated secretory organelle quantifications using CellProfiler

13

14 Corresponding author:

15 Dr. Ruben Bierings, Department of Hematology, Erasmus University Medical Center,  
16 Rotterdam, The Netherlands. e-mail: [r.bierings@erasmusmc.nl](mailto:r.bierings@erasmusmc.nl)

17

18

19 Word count abstract: 193 Figure count: 6

20 Word count: 5278 Number of references: 14

21

22

23 Key words: CellProfiler, organelle, quantification, VWF, WPB, Rab27A, ECFC

- 24 Abbreviations:
- 25 OP – OrganelleProfiler
- 26 OCP – OrganelleContentProfiler
- 27 ECFC – Endothelial colony forming cells
- 28 WPB – Weibel-Palade body
- 29 VWF – Von Willebrand factor
- 30 VWD – Von Willebrand disease
- 31 A.U. – Arbitrary intensity units

## 32 **Abstract**

33 One of the most used and versatile methods to study number, dimensions, content and localization of  
34 secretory organelles is confocal microscopy analysis. However, considerable heterogeneity exists in  
35 the number, size and shape of secretory organelles that can be present in the cell. One thus needs to  
36 analyze large numbers of organelles for valid quantification. Properly evaluating these parameters  
37 requires an automated, unbiased method to process and quantitatively analyze microscopy data. Here,  
38 we describe two pipelines, run by CellProfiler software, called OrganelleProfiler and  
39 OrganelleContentProfiler. These pipelines were used on confocal images of endothelial colony forming  
40 cells (ECFC) which contain unique secretory organelles called Weibel-Palade bodies. Results show  
41 that the pipelines can quantify the cell count and size, and the organelle count, size, shape, relation to  
42 cells and nuclei, and distance to these objects. Furthermore, the pipeline is able to quantify secondary  
43 signals located in or on the organelle or in the cytoplasm. Cell profiler measurements were checked for  
44 validity using Fiji. To conclude, these pipelines provide a powerful, high-processing quantitative tool for  
45 analysis of cell and organelle characteristics. These pipelines are freely available and easily editable  
46 for use on different cell types or organelles.

47

## 48 Introduction

49 Eukaryotic cells are compartmentalized into organelles, subcellular entities separated from the  
50 cytoplasm by a limiting membrane that enable them to more efficiently carry out specialized functions  
51 in the cell, such as energy production and protein synthesis, transport and degradation. A specific class  
52 of organelles consists of secretory vesicles, which serve to temporarily store and then rapidly secrete  
53 molecules into the extracellular space on demand. Secretory organelles are vital to maintaining  
54 homeostasis, as they allow a cell to communicate with other, distant cells or to respond to immediate  
55 changes in its environment, such as in the case of injury or when encountering pathogens. Their  
56 function is often defined by the content that is secreted, which is cell type and context specific, and  
57 depends on a sufficient magnitude of release, which directly relates to the number and dimensions of  
58 the secretory organelles that can undergo exocytosis. Moreover, the intracellular location of secretory  
59 organelles in relation to their site of biogenesis (i.e. the Golgi apparatus), filaments of the cytoskeleton  
60 and the plasma membrane also indirectly determines their exocytotic behavior.

61 Weibel-Palade bodies (WPBs) are cigar-shaped endothelial cell specific secretory organelles that  
62 contain a cocktail of vasoactive molecules that are released into the circulation in response to vascular  
63 injury or stress (1). WPBs owe their typical elongated morphology to the condensation of its main cargo  
64 protein, the hemostatic protein Von Willebrand factor (VWF), into parallel organized tubules that unfurl  
65 into long platelet-adhesive strings upon release (2). The size and shape of WPBs are of interest from a  
66 biological and medical perspective as they correlate with the hemostatic activity of the VWF strings that  
67 are released (3) and can be reflective of disease states, such as in the bleeding disorder Von Willebrand  
68 Disease (VWD) (4). A model frequently used to study the pathophysiology of vascular diseases like  
69 VWD is the Endothelial Colony Forming Cell (ECFC). A major advantage of this model is that ECFCs  
70 can be derived from whole blood of patients, which allows analysis of patient endothelial cell function,  
71 WPB morphology and secretion *ex vivo*. However, substantial phenotypic heterogeneity can exist  
72 between ECFCs (5, 6), which stresses the need for robust quantitative analytical methods to evaluate  
73 their phenotype.

74 One of the most used and versatile methods to study number, dimensions, content and localization of  
75 secretory organelles is confocal microscopy analysis. However, as with all biological samples,  
76 considerable variability exists in the number, size and shapes of secretory organelles that can be

77 present in the cell. One thus needs to analyze large numbers of organelles while ideally collecting this  
78 information in such a manner that it can be analyzed in a cell-by-cell manner. The crowded intracellular  
79 environment in combination with optical and immunostaining limitations presents an additional,  
80 technical challenge to separate individual organelles, which often precludes analysis on single organelle  
81 detail. Proper evaluation of these parameters requires an automated, unbiased method to process and  
82 quantitatively analyze microscopy data.

83 Here we describe 2 pipelines developed in CellProfiler (7), a free, easy to use image analysis software  
84 that uses separate module-based programming, for the identification, quantification and morphological  
85 analysis of secretory organelles within endothelial cells. The automated analysis pipeline  
86 OrganelleProfiler (OP) segments cells, WPBs, nuclei and cell membranes from microscopy images,  
87 quantifies number, location, size and shape of WPBs and extracts these data per cell and relative to  
88 the location of nucleus and perimeter of the cell. The function of the OrganelleProfiler pipeline is  
89 demonstrated by automated analysis of 2 previously established phenotypic classes of healthy donor  
90 ECFCs (6), which identifies clear differences in number, length, eccentricity and intracellular localization  
91 of WPBs. A second pipeline, called OrganelleContentProfiler (OCP), expands on the capabilities of the  
92 OrganelleProfiler by offering additional modules to measure the intensity of proteins of the secretory  
93 pathway both inside and outside the WPB. As an example we analyzed the presence of the small  
94 GTPase Rab27A on WPBs (8-10) and used protein disulfide isomerase (PDI), a marker for the  
95 endoplasmic reticulum, as a control as this marker is not present on WPBs.

96 Our CellProfiler pipelines provide robust and unbiased quantitative analysis tools for WPB  
97 morphometrics and can, with minimal adaptation, also be used to obtain quantitative data for other  
98 organelles and/or other cellular systems.

## 99 **Materials & Methods**

### 100 **Endothelial Colony Forming Cells and Ethical Approval**

101 General cell culture of Endothelial Colony Forming Cells (ECFCs) was performed as described (5). The  
102 study protocol for acquisition of the ECFCs was approved by the Leiden University Medical Center  
103 ethics review board. Informed consent was obtained from three subjects in accordance with the  
104 Declaration of Helsinki. Healthy participants were 18 years or older and had not been diagnosed with  
105 or known to have VWD or any other bleeding disorder. The ECFCs used in this study have previously  
106 been classified as group 1 or group 3 (6).

### 107 **Immunofluorescence of ECFCs and Image Acquisition**

108 In short, ECFCs were grown on glass coverslips (9mm) and left confluent for 5 days before fixing with  
109 70% methanol on ice for 10 minutes. Samples for OrganelleProfiler were stained with antibodies against  
110 VWF and VE-cadherin and nuclei were stained with Hoechst (S1 table for supporting information on  
111 antibodies). Samples for OrganelleContentProfiler were stained with Hoechst and antibodies against  
112 VWF, VE-cadherin and either Rab27A or PDI. After staining with appropriate fluorescently labeled  
113 secondary antibodies, coverslips were mounted using ProLong® Diamond Antifade Mountant (Thermo  
114 Fisher Scientific). Visualization of the cells for the OrganelleProfiler example was done using the  
115 Imagexpress Micro Confocal System using the 63x objective without magnification. The  
116 OrganelleContentProfiler samples were imaged using the Zeiss LSM900 Airyscan2 upright confocal  
117 microscope using the 63x oil immersion objective. For both the OrganelleProfiler and  
118 OrganelleContentProfiler images a Z-stack was made which was transformed to a maximum Z-  
119 projection.

### 120 **CellProfiler-Based pipelines for cell organelle analysis and manual** 121 **scoring with Fiji**

122 CellProfiler (version 4.2.1 at time of publication) was used, which can be downloaded from the  
123 CellProfiler website (11). Images have to be of high enough resolution that individual organelles can be  
124 identified and do not blur together. Magnification, laser intensity, detector sensitivity and other

125 acquisition parameters should be the same for each image. Image format has to be similar as well. We  
126 recommend uncompromised TIFF files. Pipelines developed are available in the Supplementary  
127 Materials (S1 and S2 file). To compare the CellProfiler measurements and validate these, manual  
128 scoring of cell count, cell surface area, WPB count, WPB length, and VWF and Rab27A intensity inside  
129 and outside the WPBs was performed using Fiji version 2.3.0 (12). Scoring was performed by using the  
130 build in scale and drawing regions of interest per cell and per WPB.

## 131 **Statistical Analysis**

132 Output data of the OrganelleProfiler pipeline was compared by Mann-Whitney test if not normally  
133 distributed data and unpaired T test with Welch's correction was performed on normally distributed data.  
134 Data of the OrganelleContentProfiler pipeline was compared with RM one way ANOVA with Geisser-  
135 Greenhouse correction. Data are presented as median with min/max boxplot. Results with p value <  
136 0.05 were considered statistically significant. P values are indicated on the graphs in the figures. Data  
137 analyses was performed using GraphPad Prism 9.3.1 (GraphPad Software, San Diego, CA, USA).

138

## 139 Results

### 140 **OrganelleProfiler (OP) – Automated identification and quantification** 141 **of nuclei, cells and secretory organelles**

142 Described here are the modules used in the OrganelleProfiler pipeline for the identification and  
143 measurement of endothelial cells, their nuclei and WPBs. The most important parameters and how  
144 these can be adjusted for use on other tissues for each module are mentioned in S3 file. Full  
145 explanations of other variables are available from the help function within the CellProfiler software or  
146 from the user manual on the CellProfiler website (11). For the development of OrganelleProfiler we  
147 used confocal images from ECFC clones from several healthy donors. These ECFCs have previously  
148 been classified into separate phenotypic groups based on cellular morphology and showed clear  
149 differences in expression of cell surface markers, proliferation and storage and secretion of VWF (6).  
150 Representative images of group 1 (top) and group 3 (bottom) ECFCs used for this study are shown in  
151 Fig 1. The CellProfiler modules that together form the OrganelleProfiler pipeline can be divided into 6  
152 steps (Fig 2), which are described below.

153 **Fig 1. Representative images of healthy ECFC controls belonging to previously classified**  
154 **groups based on morphology (6).** Group 1 ECFCs (top) and group 3 ECFCs (bottom) were stained  
155 with Hoechst (blue) and antibodies against VE-cadherin (red) and VWF (green). Scale bar represents  
156 50  $\mu\text{m}$ . Images were taken with a 63x objective.

157 **Fig 2. OrganelleProfiler: Quantitative and qualitative analysis of cells and cell secretory**  
158 **organelles.** Left, flowchart of the modules within the OrganelleProfiler pipeline. I) Input of images and  
159 splitting of channels. II) Smoothing (top), thresholding (middle) and identification of the nuclei (bottom).  
160 Every different color indicates a different object. III) Smoothing of the cell membrane (top), identification  
161 of the cells (middle) and identification of cell membranes (bottom) as objects. IV) VWF signal rescaling  
162 and enhancement (top) and identification of WPB objects (bottom). V) Relating WPBs and Cells as child  
163 and parent respectively. Same colored objects indicate a relationship to the same cell. VI) Generated  
164 output image overlaying the outline of the nuclei (blue), cells (red), and WPBs (green) objects on the  
165 VWF channel. With the addition of the cell number (purple).



166

## 167 **Step I – Input of images**

168 Firstly, images of interest are imported into the software. In this example, 5 images from two groups of  
169 ECFCs were compared. Each image has 3 channels, 1 for the nuclei staining (Hoechst), one for cell  
170 membrane staining (VE-cadherin) and a third channel for organelle specific staining (VWF) (Fig 1).  
171 Channels are separated at this point so that each channel is processed separately in the following  
172 steps.

## 173 **Step II, III and IV – Identification of nuclei, cell membranes, cells and organelles**

174 Second, the nuclei staining signal is smoothed and a threshold is applied for the identification of the  
175 nuclei as objects. This object, together with the smoothed cell membrane staining signal is used in step  
176 III for the identification of the whole cell as secondary object. The nuclei are used as a starting point  
177 from which the object propagates outward in all directions until it encounters a secondary signal, in this  
178 case the smoothed cell membrane. A third object is generated using the cell object. This third object  
179 consists of only the cell membrane which is needed in the OrganelleContentPipeline. In parallel to  
180 steps II and III, step IV uses the organelle staining signal for identification of the organelles. The signal  
181 is first rescaled and the speckle and neurite features are enhanced, which yields a better separation of  
182 organelles if they are located close to, or on top of, each other. After modification, the organelles are  
183 identified as the fourth object class.

## 184 **Step V – Measurement and relating of objects**

185 All objects that are generated in step II, III and IV are measured here. Size, shape and intensity, where  
186 relevant, is measured. Organelle objects are related to the nuclei and to the cell membrane in this step  
187 as well. This yields counts of secondary objects (organelles) per primary objects (cells) and distance of  
188 the secondary object to either the nuclei or the cell membrane. Measurements that we performed on  
189 the objects are eccentricity (as indicator for round or elongated WPB morphology), length of WPBs  
190 (maximum ferret diameter) and absolute as well as relative distance of WPBs to the nuclei and the cell  
191 membrane (Fig 3A).

192 **Fig 3. Quantitative and morphological differences between ECFC control groups.** Two previously  
193 **classified ECFCs based on morphology (6)**, group 1 (green) and group 3 (red), were stained for  
194 Hoechst, VE-cadherin and VWF. Per control, 5 images were analyzed with the OrganelleProfiler  
195 pipeline. A) Graphical representation of the measurements that were performed on the objects.  
196 Eccentricity (top), length of Weibel-Palade bodies (WPBs) measured as maximum ferret diameter  
197 (middle) and distance of WPBs to the nuclei and the cell membrane was measured (bottom). Relative  
198 distance of the WPB to the nucleus in the cell was calculated as  $100\% \times (\text{distance to nucleus}) / (\text{distance}$   
199  $\text{to nucleus} + \text{distance to cell membrane})$ . B) Cell count per image. C) The cell area ( $\mu\text{m}^2$ ) per cell of all  
200 5 images pooled ( $n = 188$  in group 1 and  $n = 52$ ). D) Number of WPBs per cell. E) Distance of the WPB  
201 to the nucleus relative to their position in the cell in percentage. F) Mean WPB length per cell in  $\mu\text{m}$ . G)  
202 Mean eccentricity of WPBs per cell. Data is shown as median with min/max boxplot. Mann-Whitney test  
203 was performed on not normally distributed data (D and G). Unpaired T test with Welch's correction was  
204 performed on normally distributed data (B, C, E and F); \* $p < 0.05$  \*\* $p < 0.01$ , \*\*\* $p < 0.001$ .

## 205 **Step VI – Quality control and analysis of output**

206 For quality control, all objects' outlines are overlaid on the VWF signal. This overlay allows the user to  
207 check whether the pipeline was accurate in the identification of objects. Cells are numbered so potential  
208 outliers can be easily identified and the pipeline can be adjusted if needed. The exported output can be  
209 used to quantify and perform qualitative analysis on images of interest.

210 Automated quantification using OrganelleProfiler revealed significant differences in cell count, cell area  
211 and number, size, shape and localization of WPBs between group 1 and group 3 ECFCs (Fig 3B-G).  
212 Data is shown as mean  $\pm$  standard deviation (SD). Fig 3B shows a significantly lower number of cells  
213 per image in group 3 ( $10.40, \pm 2.40$ ) compared to group 1 ( $37.60, \pm 2.80$ ) ( $p = 0.0003$ ). Logically, as all  
214 ECFCs were confluent, we observed a larger mean cell area in group 3 ( $4016 \mu\text{m}^2, \pm 2445$ ) than in  
215 group 1 ( $1143 \mu\text{m}^2, \pm 516.60$ ) (Fig 3C) ( $p < 0.0001$ ). The total number of WPBs per image was lower in  
216 group 1 compared to group 3 (not shown). Additionally, the number of WPBs per cell was significantly  
217 lower in group 3 ( $30.92, \pm 29.54$ ) than in group 1 ( $107.30, \pm 58.51$ ) ( $p < 0.0001$ ) (Fig 3D). The distance  
218 of WPBs to the nuclei relative to their position in the cell was determined and shown in Fig 3E. The  
219 relative distance was significantly lower in group 3 ECFCs ( $32.31\%, \pm 23.62$ ) when compared to group  
220 1 ( $53\%, \pm 30.10$ ) ( $p < 0.0001$ ) indicating that within the cell, WPBs were located closer to the nucleus in

221 group 3 ECFCs. Finally, the mean WPB length was lower in group 3 ( $1.10 \mu\text{m}, \pm 0.27$ ) versus ( $1.38 \mu\text{m},$   
222  $\pm 0.21$ ) in group 1 ECFCs ( $p < 0.0001$ ) and the WPBs were significantly more round in group 3 ( $0.63, \pm$   
223  $0.08$ ) versus ( $0.78 \pm 0.04$ ) ( $p < 0.0001$ ) (Fig 3F/G). The lower number of WPBs and the observation that  
224 they are smaller and rounder in group 3 when compared to group 1 could explain the decreased  
225 production and secretion of VWF observed previously (de Boer, JTH, 2020).

226 To further validate the quantitative data obtained from our automated OrganelleProfiler pipeline we also  
227 performed a manual quantification of several of these parameters using Fiji image analysis software,  
228 specifically the region of interest manager (12). One image of the group 1 ECFCs was used for the  
229 scoring. The manual scoring of the cells using the freehand selection resulted in 34 cells with a mean  
230 surface area of  $1264 \mu\text{m}^2, \pm 497.93$ . For three cells all WPBs were scored using the straight line  
231 measuring the longest distance in the WPB. In these cells the manual scoring showed a mean WPB  
232 count  $117, \pm 38.63$  and a length of  $1.57 \mu\text{m}, \pm 0.09$ . All measurements were compared with the  
233 CellProfiler measurements on the same image and none of the results differed significantly. Taken  
234 together, we can conclude that both measurements with CellProfiler and Fiji are comparable and thus  
235 CellProfiler can be used to accurately measure cells and organelles.

236

## 237 **OrganelleContentProfiler (OCP)- Automated measurement of** 238 **proteins in secretory organelles**

239 The OrganelleContentProfiler pipeline is an addition to the OrganelleProfiler pipeline. By adding 4 extra  
240 steps, secondary proteins of interest in, on or outside the organelle can be measured. For this purpose  
241 we analyzed the presence of Rab27A, a small GTPase that promotes WPB exocytosis and that is  
242 recruited to the WPB membrane during the maturation of these organelles after their separation from  
243 the Golgi complex (9, 10, 13). We also determined as a control the presence of protein disulfide  
244 isomerase (PDI), a marker for the endoplasmic reticulum which should not show specific localization in  
245 or on the WPBs (5, 14). Fig 4 shows example images of Rab27A as well as PDI co-staining in group 1  
246 healthy donor ECFCs that were used in this pipeline. The CellProfiler modules that together form the  
247 OrganelleContentProfiler pipeline can be divided into 4 steps (Fig 5), which are described below.  
248 Further details on every module are described in S3 file.

249 **Fig 4. Representative images of one healthy group 1 ECFC control belonging to previously**  
250 **classified groups based on morphology (6).** Cells were stained for Hoechst (blue), VE-cadherin  
251 (red), VWF (green) and Rab27A (top) or PDI (bottom). Scale bar represents 20  $\mu\text{m}$ . Images were taken  
252 with a 63x objective. Red arrows indicate WPBs as identified in the VWF channel and the same location  
253 in the Rab27A or PDI channel.

254 **Fig 5. OrganelleContentProfiler: Quantitative and qualitative analysis of other organelle**  
255 **proteins.** Top, flowchart of the modules within the OrganelleContentProfiler pipeline. I) Input of Rab27A  
256 (Organelle content) channel and rescaling of this channel. II) Input of primary object (Organelle) (left).  
257 and expansion of this object (right). III) Masking of the Rab27A channel using the Expanded organelle  
258 objects to leave only Rab27A signal inside the organelle (left). Identification of the Rab27A signal per  
259 WPB as object (middle) and relating these objects to the cells as child and parent respectively (right).  
260 IV) Masking of the Rab27A channel using the Expanded organelle objects to leave only Rab27A signal  
261 outside the organelle (left). Identification of the Rab27A signal in the cell as object without the  
262 WPBs(middle) and relating these objects to the cells as child and parent respectively (right). \* Identified  
263 in step IV of the OrganelleProfiler pipeline (Fig 2). \*\* Pipeline continues with step V and VI from the  
264 OrganelleProfiler pipeline.

265

## 266 **Step I – Input of an additional channel**

267 Similarly to the OrganelleProfiler, images are imported into the software. In this example, images have  
268 one additional channel containing the staining for either Rab27A or PDI. Again, channels are separated  
269 and the fourth channel is rescaled in order to view the channel in the final quality control.

## 270 **Step II – Import of organelle object identified in the OrganelleProfiler pipeline**

271 In this step, the organelle object as identified in the OrganelleProfiler pipeline is modified. The objects  
272 are initially identified using the staining for VWF, which is a cargo protein that is contained within the  
273 organelle. The secondary protein of interest, Rab27A, is a membrane protein that is located on the  
274 cytoplasmic face of the WPB membrane. To ensure full encapsulation of the Rab27A signal the object  
275 is therefore expanded by 2 pixels in all directions.

276 **Step III and IV – Identification of the secondary protein of interest “inside” and**  
277 **outside the organelle**

278 In these parallel steps, the expanded organelle objects and the rescaled secondary staining channel  
279 are used. The expanded objects are used as a mask to remove all signal of the Rab27A or PDI staining  
280 outside the organelle (step III) and inside the organelle (step IV). The remaining signal is then identified  
281 as object, resulting in two new objects containing the signal inside the organelles and outside the  
282 organelles respectively. These new objects are processed according to step V from the  
283 OrganelleProfiler including the measurements, relating, quality control and export.

284 **Step V and VI – Measurements, quality control and analysis of results**

285 In the OrganelleContentProfiler pipeline, different stainings on the same ECFC control are compared.  
286 In addition to the output from the OrganelleProfiler, the OrganelleContentProfiler provides  
287 measurements of the intensity of a secondary signal inside the organelle. Furthermore, it can quantify  
288 the cytoplasmic intensity values outside of the organelle which can be used for correction of the “inside”  
289 organelle signal. Signal intensity is noted as arbitrary intensity units (A.U.) as microscopes are not  
290 calibrated to an absolute scale.

291 We first confirmed that the number of WPBs quantified using OrganelleContentProfiler does not depend  
292 on the co-staining used (Rab27A:  $204.8 \pm 70.48$ ; PDI:  $146, \pm 56.38$ ;  $p=0.24$ ) (Fig 6A). ECFCs were  
293 stained with Hoechst and with antibodies against VE-cadherin, VWF and Rab27A or PDI . Fig 6B shows  
294 the A.U. inside and outside organelles and the A.U. inside the organelle corrected for the outside value.  
295 First, the VWF A.U. was analyzed as a measurement of a protein that is located predominantly in the  
296 WPB. The results show that the VWF A.U. values outside the WPBs was nearly zero ( $0.00076 \pm$   
297  $0.00033$ ) and differed significantly from the inside A.U. ( $0.028 \pm 0.0040$ ) ( $p=0.0016$ ) indicating that VWF  
298 is almost exclusively present in WPBs. Secondly, it was determined that the Rab27A staining shows a  
299 significantly higher A.U. inside ( $0.081 \pm 0.0085$ ) the WPBs when compared to the outside measurement  
300 ( $0.052 \pm 0.0041$ ) ( $p=0.0062$ ). From this it can be concluded that part of the Rab27A protein is present  
301 in or on the WPB. Finally, the A.U. of the PDI staining was analyzed. PDI is only present inside the  
302 endoplasmic reticulum and should not yield increased A.U. inside the WPB. Indeed, the A.U. inside

303 (0.074 ± 0.016) and outside (0.062 ± 0.0082) the organelle were similar (p=0.20), indicating that PDI is  
304 not located specifically in or on WPBs.

305 **Fig 6. Quantification of signal intensity inside cell organelles.** A group 1 ECFC control as defined  
306 previously (6) was stained with Hoechst and with antibodies against VE-cadherin, VWF and PDI or  
307 Rab27A. One image per staining was analyzed using the OrganelleContentProfiler pipeline. A) Both  
308 images had the same number of cells (n=4) and the same number of WPBs. B) the mean intensity in  
309 arbitrary intensity units (A.U.) per cell. for the PDI (left), Rab27A (middle) and VWF (right) staining. Each  
310 graph shows the measured mean intensity inside (in) the WPBs, outside (out) the WPBs and the  
311 intensity inside the WPB after correcting for the out signal (corr). Data is shown as median with min/max  
312 boxplot. RM one way ANOVA was performed with Geisser-Greenhouse correction; \*p<0.05 \*\*p<0.01,  
313 \*\*\*p<0.001.

314 Once more, to validate the quantitative data obtained by CellProfiler, we also performed a manual  
315 scoring using Fiji of the A.U. for the Rab27A and VWF staining inside and outside of all WPBs (n=199)  
316 in one cell. We observed that the results determined manually using Fiji (A.U. VWF inside = 0.039, VWF  
317 outside = 0.000029; Rab27A inside = 0.094, Rab27A outside = 0.053) lie within the same range as  
318 those determined by CellProfiler. This shows that the OrganelleContentProfiler can determine organelle  
319 specific stainings and measure the intensity of the staining corrected for the cytoplasmic value.

320

## 321 Discussion

322 Quantifying large numbers of organelles is challenging due to the density and morphological  
323 heterogeneity of the organelles. The pipelines described here can be used to overcome these  
324 challenges and can provide organelle analysis in great detail on a larger scale. The OrganelleProfiler  
325 allows for measurement of cell and nucleus quantity and shape, and organelle quantity, shape, size  
326 and location within the cell. The organelles are also related to the cells which allow for cell-by-cell  
327 analysis. This information can be used to determine differences between a heterogeneous cell  
328 population or between patient and control cells. The OrganelleProfiler pipeline has shown significant  
329 differences between group 1 and group 3 ECFC controls based on only 5 images. Once optimized for  
330 a set of images, the pipeline can analyze thousands of cells and hundreds of thousands of organelles  
331 within hours without potential bias associated with manual image processing and quantification.  
332 Furthermore, with the OrganelleContentProfiler, secondary organelle markers can be measured and  
333 quantified. We showed 3 stainings of proteins with different localizations; PDI, which is only present on  
334 the endoplasmic reticulum, Rab27A which is present in the cytoplasm, but is also trafficked to the  
335 WPBs, and VWF which is mostly present in WPBs. Using the OrganelleContentProfiler pipeline we  
336 were able to quantify these stainings and determine the localization of these proteins. It is also possible  
337 to measure other organelle stainings at the same time by duplicating modules 3 to 8 of this pipeline and  
338 adjusting these for the additional channels.

339 Finetuning of the smoothing, thresholds and enhancement of the signal is necessary to ensure correct  
340 identification of objects. For every image set, a balance must be found to prevent over and under  
341 segmentation of organelles. Despite optimization, perfect segmentation of organelles is not always  
342 possible, especially in areas where organelles are crowded together. These imperfections may lead to  
343 incorrect identification of organelles, which could play out as underestimations of WPB numbers or  
344 overestimation of WPB dimensions. However, as all images are analyzed by the same pipeline, this  
345 error is expected to occur to a similar extent in all samples. One point of improvement on the  
346 OrganelleContentProfiler pipeline could be the correction of the organelle secondary staining with the  
347 intensity levels directly surrounding the organelle instead of the mean intensity in the entire cytoplasm.  
348 This was not possible within the CellProfiler software but could be done in data processing afterwards

349 using the MeasureObjectIntensityDistribution module and relating this to the distance of WPBs to the  
350 nucleus (7).

351 A comparison with manual scoring using Fiji was performed to check the validity of the results generated  
352 by our automated pipelines. We generally found that the results obtained with OrganelleProfiler and  
353 OrganelleContentProfiler correspond very well with manual quantifications using Fiji, although subtle  
354 differences were found for two parameters. First, the maximum ferret diameter is calculated based on  
355 the smallest convex hull that is created around the WPB. The manual scoring measured the length of  
356 the WPB in a line and not as the inside of a convex hull. This could cause the slight difference in length  
357 as measured between CellProfiler and Fiji. Second, VWF and Rab27A intensities inside WPBs as  
358 determined by manual scoring was slightly higher than from the OrganelleContentProfiler  
359 measurements. Possibly, the outlines that were drawn around WPBs manually were more strict than  
360 those generated by OrganelleContentProfiler, because the human eye is less capable at detecting the  
361 very small changes in signal intensity near the edges of the organelles. As such, the signal intensities  
362 in these edges may have not been included in the manual analysis, resulting in a higher mean value  
363 per WPB.

364 To conclude, the OrganelleProfiler and OrganelleContentProfiler pipelines provide powerful, high-  
365 processing quantitative tools for analysis of cell and organelle count, size, shape, location and content.  
366 These pipelines were created with the purpose of analyzing morphometric parameters of WPBs in  
367 endothelial cells, but they can be easily adjusted for use on different cell types or organelles. This can  
368 be especially useful for analysis of large datasets where manual quantification of organelle parameters  
369 would be unfeasible.

370





## 372 **Acknowledgements**

373 The SYMPHONY consortium, which aims to orchestrate personalized treatment in patients with  
374 bleeding disorders, is a unique collaboration between patients, health care professionals, and  
375 translational and fundamental researchers specializing in inherited bleeding disorders, as well as  
376 experts from multiple disciplines. It aims to identify best treatment choice for each individual based on  
377 bleeding phenotype. To achieve this goal, work packages (WP) have been organized according to 3  
378 themes (e.g. Diagnostics [WPs 3 and 4], Treatment [WPs 5-9], and Fundamental Research [WPs 10-  
379 12]). Principal investigator: M.H. Cnossen; project manager: S.H. Reitsma.

380

### 381 **Authorship Contributions**

382 SNJL and RJD performed research, developed quantification methods and analyzed data; SNJL, JE,  
383 and RB designed the research and wrote the paper.

384

## References

- 385 1. Schillemans M, Karampini E, Kat M, Bierings R. Exocytosis of Weibel-Palade bodies: how to  
386 unpack a vascular emergency kit. *J Thromb Haemost.* 2019;17(1):6-18.
- 387 2. Valentijn KM, Sadler JE, Valentijn JA, Voorberg J, Eikenboom J. Functional architecture of  
388 Weibel-Palade bodies. *Blood.* 2011;117(19):5033-43.
- 389 3. Kat M, Margadant C, Voorberg J, Bierings R. Dispatch and delivery at the ER-Golgi interface:  
390 how endothelial cells tune their hemostatic response. *Febs j.* 2022.
- 391 4. Valentijn KM, Eikenboom J. Weibel-Palade bodies: a window to von Willebrand disease. *J*  
392 *Thromb Haemost.* 2013;11(4):581-92.
- 393 5. de Jong A, Weijers E, Dirven R, de Boer S, Streur J, Eikenboom J. Variability of von Willebrand  
394 factor-related parameters in endothelial colony forming cells. *J Thromb Haemost.* 2019;17(9):1544-  
395 54.
- 396 6. de Boer S, Bowman M, Notley C, Mo A, Lima P, de Jong A, et al. Endothelial characteristics in  
397 healthy endothelial colony forming cells; generating a robust and valid ex vivo model for vascular  
398 disease. *J Thromb Haemost.* 2020;18(10):2721-31.
- 399 7. Stirling DR, Swain-Bowden MJ, Lucas AM, Carpenter AE, Cimini BA, Goodman A. CellProfiler 4:  
400 improvements in speed, utility and usability. *BMC Bioinformatics.* 2021;22(1):433.
- 401 8. Hannah MJ, Hume AN, Arribas M, Williams R, Hewlett LJ, Seabra MC, et al. Weibel-Palade  
402 bodies recruit Rab27 by a content-driven, maturation-dependent mechanism that is independent of  
403 cell type. *J Cell Sci.* 2003;116(Pt 19):3939-48.
- 404 9. Bierings R, Hellen N, Kiskin N, Knipe L, Fonseca AV, Patel B, et al. The interplay between the  
405 Rab27A effectors Slp4-a and MyRIP controls hormone-evoked Weibel-Palade body exocytosis. *Blood.*  
406 2012;120(13):2757-67.
- 407 10. Kat M, Bürgisser PE, Janssen H, De Cuyper IM, Conte IL, Hume AN, et al. GDP/GTP exchange  
408 factor MADD drives activation and recruitment of secretory Rab GTPases to Weibel-Palade bodies.  
409 *Blood Adv.* 2021;5(23):5116-27.
- 410 11. Institute B. CellProfiler 2022 [<https://cellprofiler.org/citations>].
- 411 12. Schindelin J, Arganda-Carreras I, Frise E, Kaynig V, Longair M, Pietzsch T, et al. Fiji: an open-  
412 source platform for biological-image analysis. *Nature Methods.* 2012;9(7):676-82.
- 413 13. Zografou S, Basagiannis D, Papafotika A, Shirakawa R, Horiuchi H, Auerbach D, et al. A  
414 complete Rab screening reveals novel insights in Weibel-Palade body exocytosis. *J Cell Sci.* 2012;125(Pt  
415 20):4780-90.
- 416 14. Kat M, Karampini E, Hoogendijk AJ, Bürgisser PE, Mulder AA, Van Alphen FPJ, et al. Syntaxin 5  
417 determines Weibel-Palade body size and von Willebrand factor secretion by controlling Golgi  
418 architecture. *Haematologica.* 2022;107(8):1827-39.

419

## 420 **Supporting information**

421 **S1 table. Supporting information on antibodies**

422 **S1 file. OrganelleProfiler pipeline**

423 **S2 file. OrganelleContentProfiler pipeline**

424 **S3 file. Detailed guide per module of the OP and OCP pipelines**

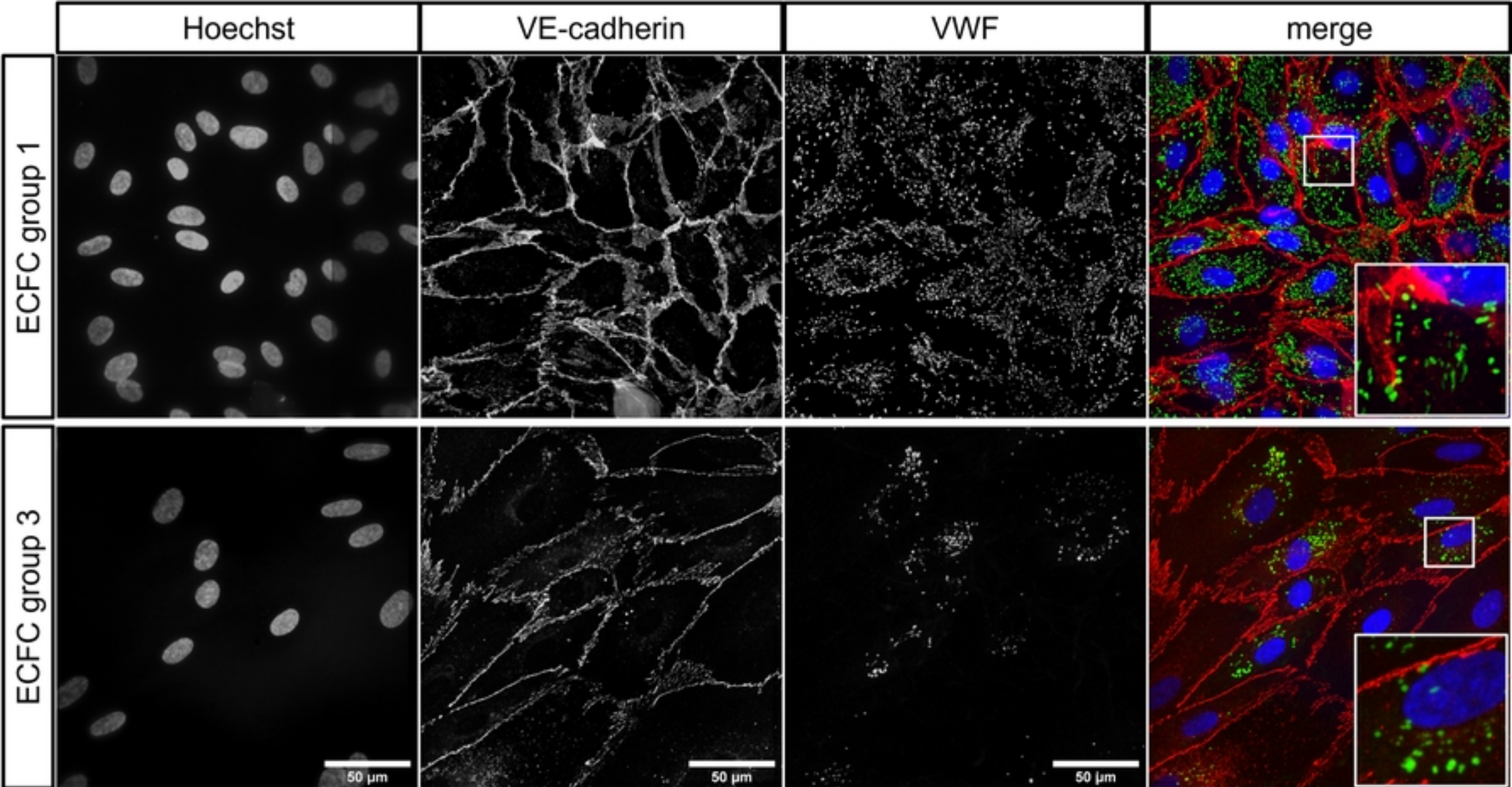


Figure 1



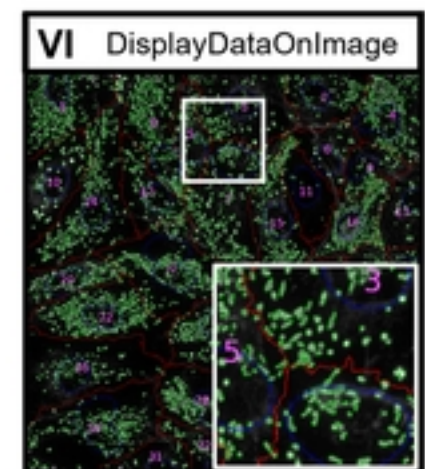
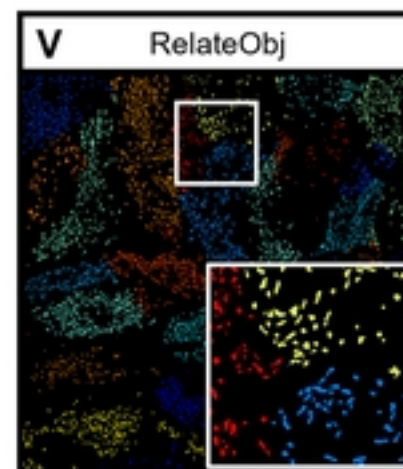
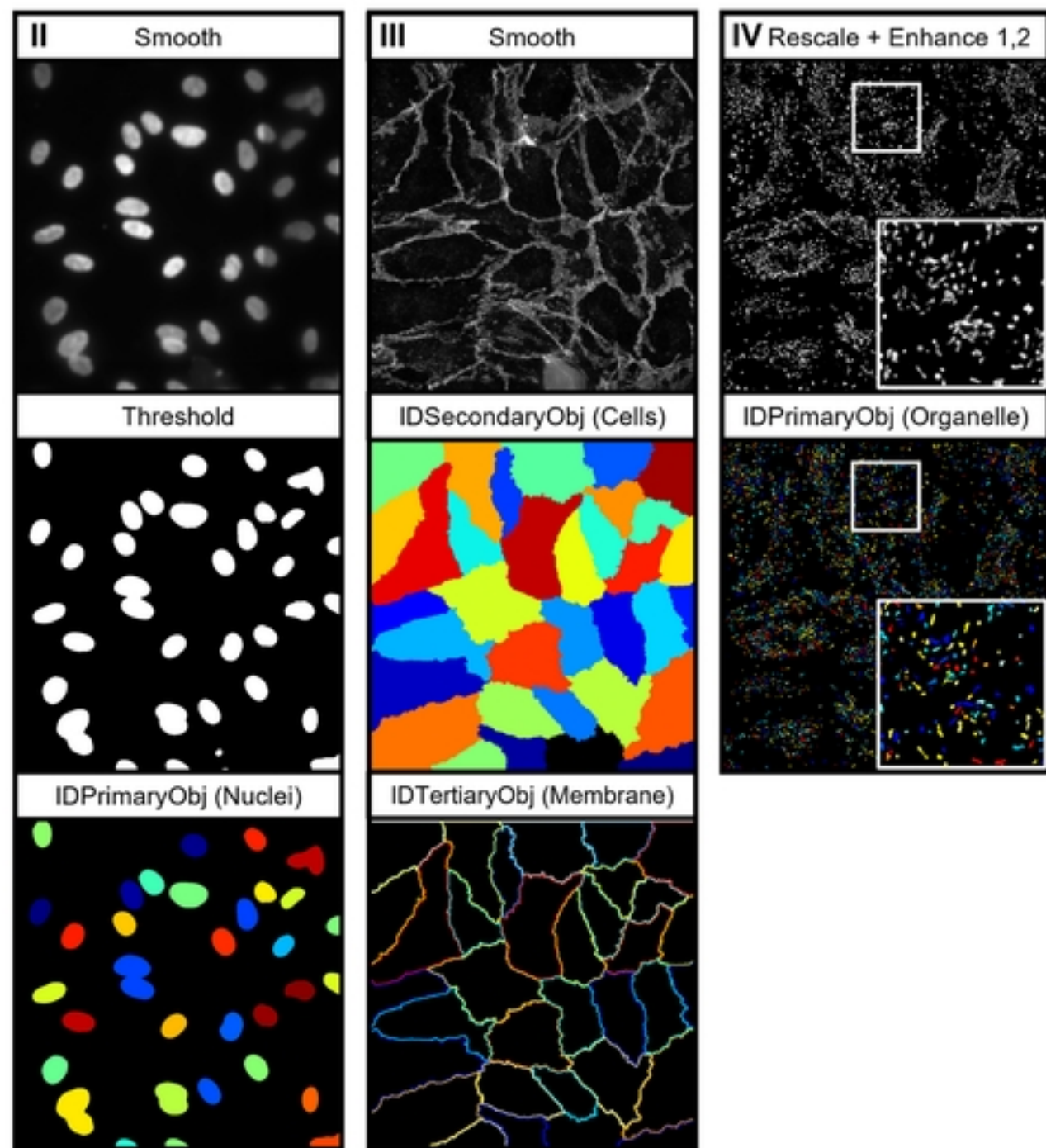
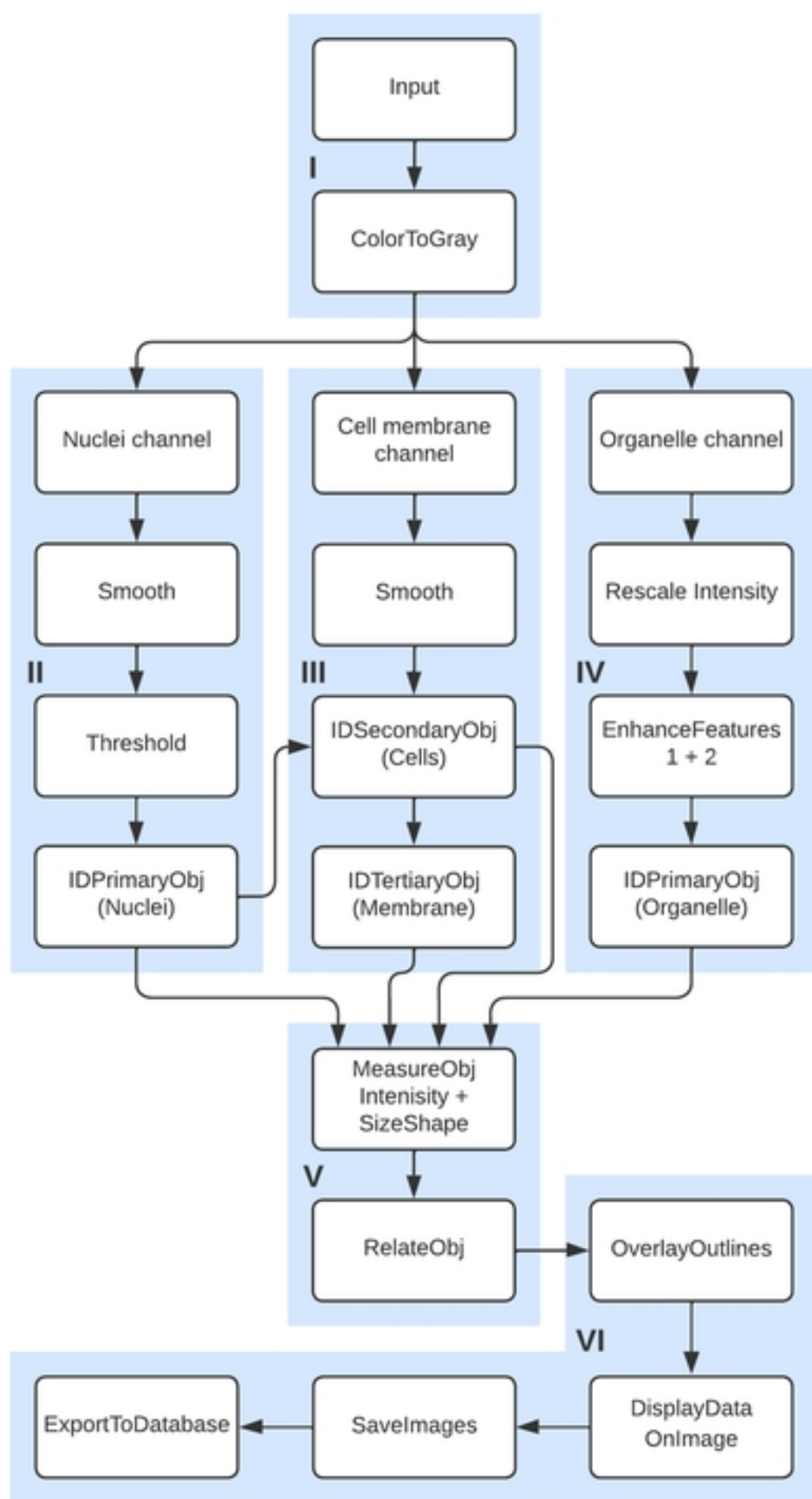


Figure 2

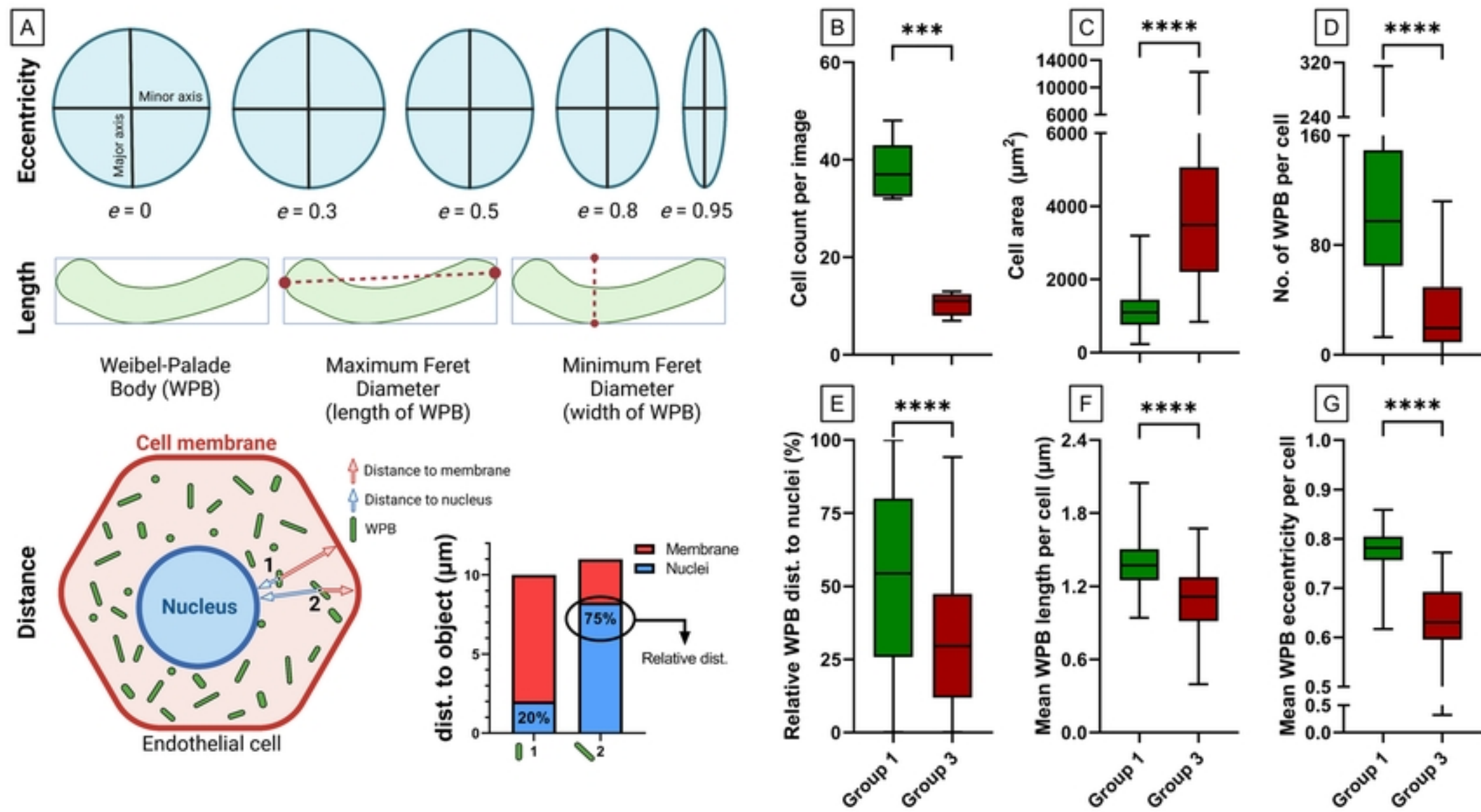


Figure 3



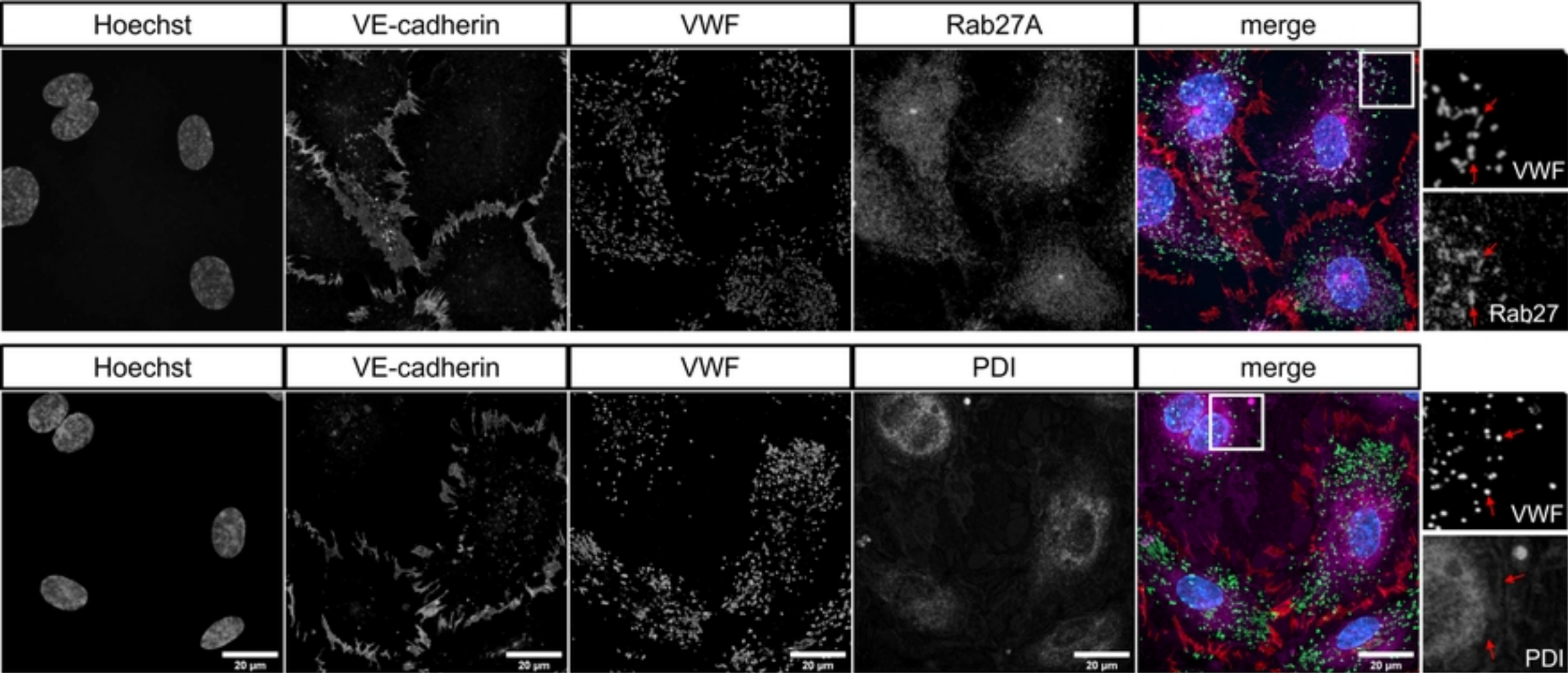


Figure 4

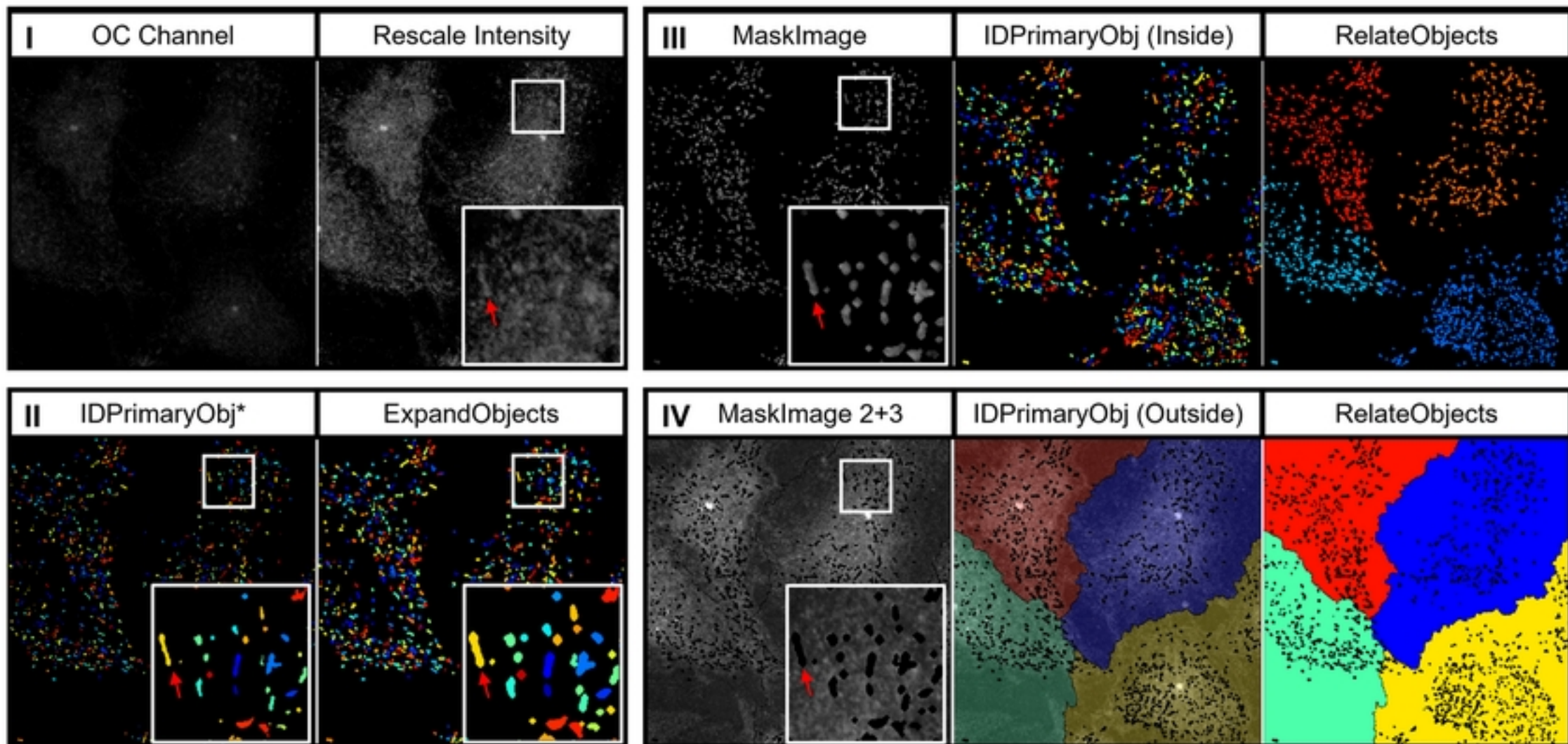
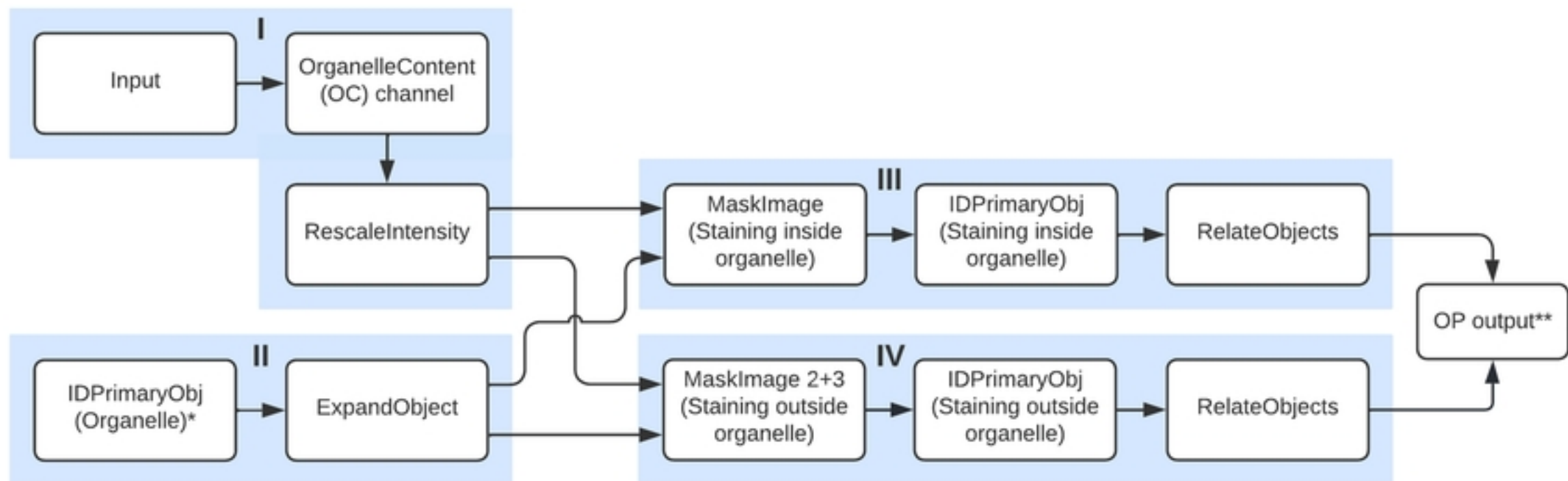


Figure 5



